Polymer Journal, Vol. 24, No. 4, pp 323—337 (1992)

The Main SAXS Features of Gamma-Irradiated Graft Copolymer of Methyl Methacrylate onto Nylon-6 Fibre Using Correlation Functions

T. MISRA, S. S. KHUNTIA, V. H. BUCH,* and T. PATEL

Department of Physics, Regional Engineering College, Rourkela-769 008, Orissa, India

(Received June 24, 1991)

ABSTRACT: The small-angle X-ray scattering (SAXS) technique was used to investigate various macromolecular structural parameters of gamma-irradiated graft copolymers of methyl methacrylate (MMA) onto Nylon-6 fibres that were further subjected to different doses of gamma-rays to study the effects of radiation. It has been observed that SAXS profiles of various samples undergo drastic change with increase in dose and also they deviate from Porod's Law, indicating that they can be classified under non-ideal two phase structure characterized by continuous variation of electron density at the phase boundary. The theories developed by Vonk and Ruland for non-ideal two phase structures have been applied to calculate various macromolecular parameters. The three and one-dimensional correlation functions have been computed from the background corrected SAXS profiles and various parameters like the width of the transition layer, the average periodicity transverse to the layer, the specific inner surface, the length of coherence, the transversal lengths in matter and in void, the range of inhomogeneity, the volume fractions of matter and void, the volume fraction of transition layer and characteristic number have been determined.

KEY WORDS Duffuse Boundary Width / Linear Gradient Model / One- and Three-Dimensional Correlation Functions / Break Down of Molecules (Degradation) / Transverse Periodicity / Inter-Domain Spacing /

Small-angle X-ray scattering (SAXS) profiles obtained from ideal two-phase systems with sharp boundaries have been treated by Porod.[1,2] The limiting behaviour of the scattered X-ray intensity at large values of s ($s=2\sin\theta/\lambda$), predicts a decrease in intensity proportional to the reciprocal of third power of s:

$$\lim_{s\to\infty}[\tilde{I}_p(s)]=\frac{K_p}{s^3} \qquad (1)$$

where s is the coordinate in Fourier or reciprocal space and K_p is known as the Porod–Law constant. Equation 1 is Porod's Law. $\tilde{I}_p(s)$ is smeared out SAXS intensity. The above equation leads to the conclusion that the product $\tilde{I}_p(s)\cdot s^3$ at large s attains a constant value K_p where

$$K_p=(S/V)Q/8\pi^3\phi_1\phi_2=Q/2\pi^3 l_p$$

and is an important parameter containing information on certain structural parameters of the system. Here (S/V) is the area of interface per unit volume, ϕ_1 and ϕ_2 are the volume fractions of the phases, Q is the well known Porod's invariant[1,2] and l_p is the Porod inhomogeneity length, a parameter which serves as a measure of the average size of the phases. Due to geometrical constraints of the measuring instruments, it is not possible

* Present address: *Centre of Advanced Studies (Physics), Bombay University, Department of Chemical Technology, Matunga, Bombay 40° 019, India.*

to measure scattered intensity at relatively higher scattering angles. In such cases, Porod's Law relation (1) affords a suitable method of extrapolation of the scattered intensity to regions inaccessible due to geometrical construction. This extrapolation permits calculation of Q, a quantity proportional to the volume fraction and electron density difference of the phases, and also the correlation function, $C(r)$, a function which contains informations regarding the shape and size of the phases.

Work on polymers often exhibits systematic deviation from Porod's Law. The product $\tilde{I}_p(s)\cdot s^3$ does not lead to a constant value at large s causing enhancement of scattering at high angles leading to a positive slope of $\tilde{I}(s)\cdot s^3$ *versus* s^2, known as positive deviation from Porod's Law. However, there are cases where the existence of a diffuse phase boundary results in depletion of high-angle scattering leading to a negative slope for a similar plot. These effects are referred to as negative deviation from Porod's Law predicted by Helfand[3] and Helfand and Tagami[4] on the basis of thermodynamic considerations. Similar deviation is also expected in semi-crystalline polymers due to crystal-surface irregularities. This diffuse boundary width is of great interest as it is expected to affect the mechanical properties of heterogeneous materials.[5]

Ruland[6] has modified Porod's Law to include the effect of deviation and put forward methods to determine the density fluctuation and width of the diffuse interface known as the width of the transition layer. Vonk[7] has developed practical aspects of Ruland method which have been rigorously followed in this work. Porod's law in terms of a model containing two phases having diffuse boundary layer in which density varies irregularly from one phase to the other is a linear gradient model.

EXPERIMENTAL

Soon after the synthesis of Nylon-6 in 1929 it has played very important roles among all the man-made fibres. The versatility of Nylon-6 can be judged by its large scale use in the form of filament yarns and staple fibre yarns for the manufacturer of carpets, tyre cords, apparel, hosiery upholstery, seat belts, parachute ropes and industrial cords etc.

In recent years radiation-induced grafting of Nylon has received higher priority.[8-10] Radiation induced graft copolymers of methyl methacrylate (MMA) onto Nylon-6 were obtained from Nayak[11] for our study. These polymers are synthesized in the Laboratory of Polymers and Fibres, Department of Chemistry, Ravenshaw College, Cuttack, Orissa, India. Investigation by other workers shows that high energy radiation like X-rays and gamma-rays results either in the break down of molecules leading to degradation or in the formation of new molecules causing further polymerization or cross-linking, thereby modifying properties like crease-resistance, water repellency, flame retardancy, antisoiling etc. of the fibre. In our present work we took fibres with seventy six percent graft yield (designated as MMA-1) which was further irradiated by 3 Mrad and 9 Mrad gamma-radiation henceforward was designated as MMA-1 (3 Mrad) and MMA-1 (9 Mrad) respectively. In view of their importance, we studied various micro and macromolecular parameters of graft copolymers of Nylon-6. The aim of the present paper is to show the effects of gamma-radiation on MMA-1 by using SAXS technique.

APPARATUS AND EXPERIMENTAL METHOD

SAXS measurements were made at Center of Advanced Studies (Physics), Bombay University, Department of Chemical Technology, Matunga, Bombay, India by Means of a Compact Kratky Camera (Anton Paar K.G. A-8054) using a Philips PW 1729 X-ray generator with a copper target operated at 40 kV and 30 mA with the following adjust-

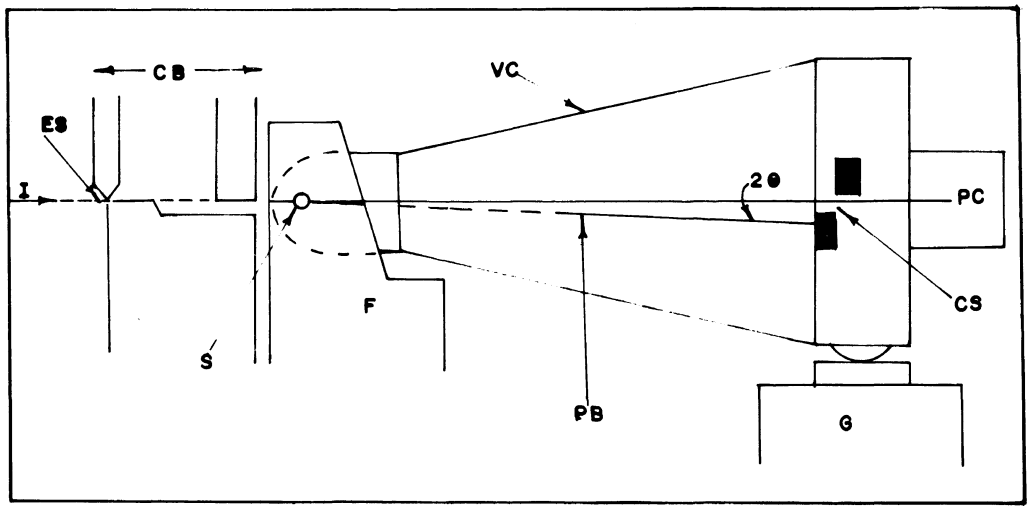

Figure 1. Schematic diagram of the Kratky camera (not to scale): I, incident X-ray beam; ES, entrance slit; CB, collimation block; S, sample; F, fork; VC, vacuum chamber; PB, primary beam; G, electronic goniometer; CS, counter slit; PC, proportional counter.

ments. The registration device used was a proportional counter. The entrance slit and counter slit attached to the Kratky camera were adjusted at 150 μm and 375 μm respectively. Monochromatic Cu-K_α ($\lambda = 1.54$ A°) radiation was obtained using a nickel filter of 10 μm thickness and used to irradiate MMA-1 fibers packed in Mark capillary tube of 1 mm diameter and aligned parallel to the X-ray beam and also perpendicular to it. The camera adjustment was checked by a lupolen sample supplied by the manufacturer. X-rays enter the evacuated space through a 0.25 mm beryllium window at the front side and scattered radiation emerges out of a similar window at the opposite side. The entire radiation path between these two windows runs through a vacuum of about 1/2 mbar, thereby avoiding parasitic scattering by air and windows as reported by Hendricks.[12] The intensity data of the empty Mark capillary was recorded earlier before collecting the intensity data of various samples. The sample to counter distance was maintained at 20 cm and room temperature was maintained at 22.5$\pm$0.5°C by an air conditioner. The schematic diagram of the compact Kratky camera used is shown in Figure 1.

THEORY

The salient features of some of the practical aspects proposed by Ruland[6] and modified by Vonk[7] are outlined here. A general relation involving the mean square electron density gradient and applicable to structure having a diffuse phase boundary characterized by continuous electron density variation is given by

$$\eta(r) = \int_0^\infty F(s)\exp(2\pi i r \cdot s)\mathrm{d}v_s = T_f(F(s)) \quad (2)$$

where $F(s)$ is the amplitude of the scattered X-rays, $\eta(r)$ is the deviation of electron density from the mean value, r is a vector in real space with coordinates x, y, z; s is a vector in reciprocal space with coordinates u, v, w; $\mathrm{d}v_s = \mathrm{d}u \cdot \mathrm{d}v \cdot \mathrm{d}w$ and T_f is Fourier transformation operator.

Differentiation of $\eta(r)$ with respect to x gives:

$$\frac{\partial \eta}{\partial x} = T_f(2\pi i u F(s)) = T_f(T(s)) \quad (3)$$

where $T(s)=2\pi iuF(s)$. Application of Parseval's theorem to (3) gives:

$$\int_0^\infty \left|\frac{\partial\eta}{\partial x}\right|^2 \mathrm{d}v_r = \int_0^\infty |T|^2 \mathrm{d}v_s \qquad (4)$$

where $\mathrm{d}v_r = \mathrm{d}x\cdot\mathrm{d}y\cdot\mathrm{d}z$. Similar expressions are found when $\eta(r)$ is differentiated with respect to y and z. Replacing $u^2+v^2+w^2$ by $|s|^2$ and $(\partial\eta/\partial x)^2+(\partial\eta/\partial y)^2+(\partial\eta/\partial z)^2$ by $|\mathrm{grad}\,\eta|^2$ one gets:

$$4\pi\int_0^\infty |s|^2 I(s)\mathrm{d}v_s = \int_0^\infty |\mathrm{grad}\eta|^2 \mathrm{d}v_r$$

which for isotropic structures reduces to

$$16\pi^3\int_0^\infty s^4 I(s)\mathrm{d}s = \int_0^\infty |\mathrm{grad}\,\eta|^2 \mathrm{d}v_r \qquad (5)$$

where $I(s)$ is desmeared intensity in absolute units. The above equation can be considered as parallel to the well known Porod's invariant relation

$$Q=4\pi\int_0^\infty s^2 I(s)\mathrm{d}s = \int_0^\infty \eta^2 \mathrm{d}v_r \qquad (6)$$

In cases when absolute intensities are not available, the ratio of eq 5 and 6 gives a very useful parameter

$$R=\frac{\langle|\mathrm{grad}\,\eta|^2\rangle}{\langle\eta^2\rangle}=4\pi^2\frac{\int_0^\infty s^4 I(s)\mathrm{d}s}{\int_0^\infty s^2 I(s)\mathrm{d}s}$$

$$=6\pi^2\frac{\int_0^\infty s^3\tilde{I}(s)\mathrm{d}s}{\int_0^\infty s\tilde{I}(s)\mathrm{d}s} \qquad (7)$$

where $I(s)$ is the desmeared intensity in arbitrary units and $\tilde{I}(s)$ is the smeared out intensity corresponding to infinite slit optics. The parameter R plays an important role in the characterization of structures. In an ideal two-phase structure the gradient at the phase boundary is infinity and consequently R goes to infinity. The case where the minimum value of $R=4\pi^2 s_0^2$ and the intensity function $I(s)$ contains a single peak at $s=s_0$, such an intensity function is obtained from a randomized layer structure in which the electron density perpendicular to the layers fluctuates according to a sine function.

To obtain the relation between R and correlation function $C(r)$ the equation

$$C(r)=\frac{\int_0^\infty I(s)\exp(2\pi ir\cdot s)\mathrm{d}v_s}{\int_0^\infty I(s)\mathrm{d}v_s}$$

is differentiated twice with respect to x. In the limit $r=0$ the above equation gives:

$$(\partial^2 C(r)/\partial x^2)_{r=0} = -4\pi^2\frac{\int_0^\infty u^2 I(s)\mathrm{d}v_s}{\int_0^\infty I(s)\mathrm{d}v_s}$$

For isotropic sample the above equation is found to be equivalent to

$$(\mathrm{d}^2 C(r)/\mathrm{d}r^2)_{r=0} = -\frac{4\pi^2}{3}\frac{\int_0^\infty s^4 I(s)\mathrm{d}s}{\int_0^\infty s^2 I(s)\mathrm{d}s}$$

which when compared with (7) yields:

$$R=-3(\mathrm{d}^2 C(r)/\mathrm{d}r^2)_{r=0} \qquad (8)$$

However whenever R is determined from the correlation function care must be taken to avoid experimental error at the tail of the scattering curve as the correlation function in the origin is very sensitive to such error as pointed out by Caulfield and Ullman.[13]

Since the intensity of the scattered X-rays is measured as a function of x the above relations written in terms of s, the coordinate in reciprocal space, are converted in terms of x, where $s=2\theta/\lambda=x/\lambda a$, since $2\theta=x/a$, where θ is the scattering angle.

The conversion of above equations in terms of x have been carried out by Misra *et al.*[14]

which are as follows:

$$R = 3/2(2\pi/\lambda a)^2 \int_0^\infty x^3 \tilde{I}(x)\mathrm{d}x \Big/ \int_0^\infty x\tilde{I}(x)\mathrm{d}x \tag{9}$$

The higher values of exponent of x for which Porod's Law fails to allow the integrals of eq 9 to converge and gives a finite R value consistent with a non-ideal two-phase structure. According to the theories of Debye and Bueche[15] and Porod[1] for two-phase systems, the smeared out invariant of a scattering profile is independent of the shape and size of the particles responsible for scattering and is proportional to $\langle \Delta\eta \rangle^2$ where $\Delta\eta$ is the electron density difference between the two phases.

Mering and Tchoubar[16] put forward a method of calculating three-dimensional correlation function, $C(r)$ from the smeared out intensity $\tilde{I}(s)$ which reads as:

$$C(r) = \int_0^\infty s\tilde{I}(s)J_0(2\pi rs)\mathrm{d}s \Big/ \int_0^\infty s\tilde{I}(s)\mathrm{d}s \tag{10}$$

where J_0 is the Bessel function of zero order and of the first kind. The function $C(r)$ is obtained from the smeared out intensity $\tilde{I}(s)$ where slit correction for infinite slit geometry given by the relation:

$$\tilde{I}(s) = \int_{-\infty}^{\infty} I(s^2 + t^2)^{1/2}\mathrm{d}t$$

is incorporated[16a] and contained in Bessel function J_0 (t is an arbitrary variable representing the slit length). When variable x is used, eq 10 reduces to:

$$C(r) = \int_0^\infty x\tilde{I}(x)J_0(2\pi rx/(\lambda a))\mathrm{d}x \Big/ \int_0^\infty x\tilde{I}(x)\mathrm{d}x \tag{11}$$

The value of diffuse boundary thickness, E can be obtained from the three-dimensional correlation function normalized to unity at the origin in real space. The relation derived by Vonk[7] for the calculation of width of transition layer, E is

$$E = -4/R(\mathrm{d}C(r)/\mathrm{d}r)_{r=E_v} \tag{12}$$

To compute E, it is necessary to calculate the values of $C(r)$ for various values of r in real space.

For a layer structure, Kortleve and Vonk[17] made use of the one-dimensional correlation function, $C_1(y)$ where $C_1(y)$ according to Mering and Tchoubar[16] is given by

$$C_1(y) = \int_0^\infty s\tilde{I}(s)(J_0(z) - zJ_1(z))\mathrm{d}s \Big/ \int_0^\infty s\tilde{I}(s)\mathrm{d}s \tag{13}$$

In terms of x variable, the above relation can be expressed as

$$C_1(y) = \int_0^\infty x\tilde{I}(x)(J_0(z) - zJ_1(z))\mathrm{d}x \Big/ \int_0^\infty x\tilde{I}(x)\mathrm{d}x \tag{14}$$

Where $z = 2\pi xy/a$ and J_1 is the Bessel function of first order and of the first kind. In reality, however, the scattering profile is isotropic.[18] That is, the lamellae have limited coherence and can be thought of as lamellar bundles oriented equally in all directions. The scattering profile then contains information related to distance correlations averaged over all directions. Information pertaining to spatial correlations perpendicular to the lamellae may be obtained by realizing that the scattered intensity is spread out equally over the surface area of spheres in reciprocal space.

As suggested by Vonk[7] the position of the first subsidiary maximum in the one-dimensional correlation function $C_1(y)$ gives the value of periodicity, D, transverse to the layers. Using Vonk's[7] relation

$$(\mathrm{d}C_1(y)/\mathrm{d}y)_{y>E} = -1/D\langle \Delta\eta \rangle^2/\langle \eta^2 \rangle \tag{15}$$

the value of $\langle \Delta\eta \rangle^2/\langle \eta^2 \rangle$ can be estimated where $\Delta\eta$ is the electron density difference between two neighbouring phases. For calculation of D, the slope is taken at a distance

$y > E$.

For a layer structure the specific inner surface, S/V, defined as the phase boundary per unit volume of the dispersed phase, is given by Vonk[7] as

$$S/V = 2/D \tag{16}$$

For a non-ideal two phase structure, it was shown by Vonk that the relation

$$\langle \eta^2 \rangle / \langle \Delta\eta \rangle^2 = \phi_1 \phi_2 - ES/6V \tag{17}$$

holds good. The quantities ϕ_1 and ϕ_2 are the volume fractions of the two phases matter and void, respectively. To use the above equation, the phase boundary is chosen at the middle of the transition layer Taking $\phi_1 + \phi_2 = 1$, the relation (17) can be used to get individual values of ϕ_1 and ϕ_2.

Applying the method advanced by Porod[1] distance statistics can be found for determination of transversal lengths. As shown by Mittelbach and Porod[19] the transversal length of matter and void phases are given by the relations

$$\bar{l}_1 = 4\phi_1 V/S\,, \qquad \bar{l}_2 = 4\phi_2 V/S \tag{18}$$

and

$$1/\bar{l}_r = 1/\bar{l}_1 + 1/\bar{l}_2 \tag{19}$$

The range of inhomogeneity, $\bar{l}_r$ is synonimous with the concept of reduced mass in mechanics and represents an average diameter of the parts of the sample occupied by matter.

Following Mittelbach and Porod[19] the length of coherence, l_c can be estimated from the relation

$$l_c = 2\int_0^\infty C(r)\mathrm{d}r \tag{20}$$

Knowing l_c and $\bar{l}_r$ the characteristic number f_c is given by

$$f_c = 1/2(l_c/\bar{l}_r) \tag{21}$$

as defined by Porod.[1] Increase in the value of the above ratio indicates higher anisometry in the scattering system.

A second method for the determination of width of transition layer, E is given by Vonk.[7] The functional relation of $\tilde{I}(s)$ with s at the tail region of the SAXS pattern for a non-ideal two-phase system is given by

$$\tilde{I}(s) = \pi C/2(1/s^3 - 2\pi^2 E^2/3s) \tag{22}$$

where C is a constant of proportionality. The value of E becomes zero for an ideal two-phase system. In terms of x variable the above relation can be written in the form

$$\tilde{I}(x)x = \pi C/2(\lambda a)^3 x^{-2} - \pi^3 C/3(\lambda a)E^2 \tag{23}$$

The value of E can be obtained from the $\tilde{I}(x)x$ *versus* x^{-2} curve generally known as Ruland plot.

BACK GROUND CORRECTION

The SAXS pattern of any sample is associated with continuous background scattering. In polymeric material, there are several factors which give rise to such background scattering sometimes leading to positive,[20] negative[21] or constant background.[22] Wiegand and Ruland[22] have shown that background intensity may be developed as a power series in even powers of the scattering vector s. Empirical methods which are approximations to the power series have been proposed by Vonk,[7] Ruland[23] and Kortleve *et al.*[24] In such a case the experimentally observed data at large value of s can be represented by the equation

$$\tilde{I}_{bg}(s) = a + bs^n \tag{24}$$

where a and b are constant and n is an even positive integer. Konrad and Zachman[25] have shown that $\tilde{I}_{bg}(s)$ remains constant in the region where $\tilde{I}(s)$ contributes appreciably. For the above assumptions on background intensity, the value of E calculated by the methods of Vonk and Ruland leads to relatively small differences. Therefore a constant background intensity when no appreciably positive or negative deviation from Porod's law is shown

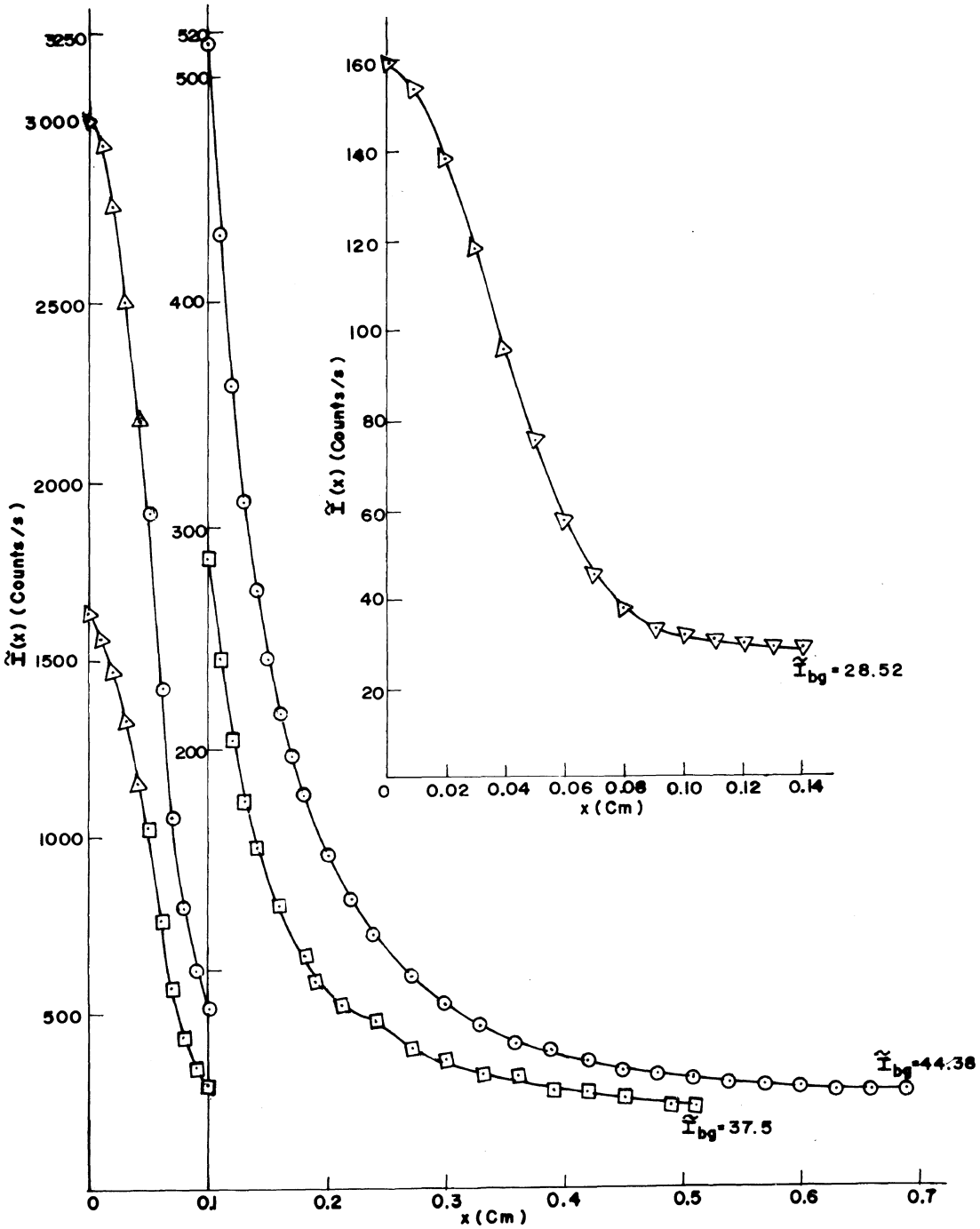

Figure 2. Smeared out scattering profiles for MMA-1 (open circles). MMA-1 (3 Mrad), open squares and MMA-1 (9 Mrad), reverse traingles magnified from 0.10. The extrapolated points are shown by △.

by SAXS profiles[14] can be deducted. In many cases as reported by Vonk[26] this background can be observed as a region of almost constant intensity at angles intermediate between small and wide angle scattering. This constant value may be subtracted from the small angle scattering. In our work constant background intensities marked as $\tilde{I}_{bg}$ in Figure 2 were deducted. The background corrected data at the tail region were subjected to the following two conditions to test their correctness. The standard deviation at this region must be below 0.5.[27] The coefficient of line of regression[28] in the same region should be nearly one. Background corrected SAXS intensities were used in our investigation. 5% statistical error was observed during the collection of intensity data. the effect of this error was eliminated in the calculation of correlation function and other parameters and error bars were plotted. The resulting limits of error due to this intensity fluctuation were calculated and included in various parameters determined by us.

CALCULATION AND RESULTS

Five intensity values in the $\tilde{I}(x)$ *versus* x curve near the origin were fitted to a Gaussian curve[29]

$$\tilde{I}(x \to 0) = p \exp(-qx^2)$$

by least square technique and the values of p for MMA-1, MMA-1 (3 Mrad) and MMA-1 (9 Mrad) were obtained as 2963.89, 1554.11, and 130.77 $J\,m^{-2}\cdot s^{-1}$, respectively and the corresponding values of q as 207.9, 206.93, and 414.77 m^{-2}, Taking the values of p and q the scattering curves for the three samples were extrapolated to zero angle. The extrapolated points for all the samples are indicated by symbol $\triangle$ in Figure 2. It may be mentioned here that the method of extrapolation has very little effect on the relevant part of the correlation functions. Neither the position nor height of first subsidiary maximum of the one-dimensional correlation function is much affected.[14] The two integrals in the relation (9) for the R parameter were calculated by numerical integration applying Simpson's one-third rule and the values of R were found to be $(15.66 \pm 0.27)10^{-4}$, $(12.72 \pm 0.23)10^{-4}$, and $(7.0 \pm 0.31)10^{-5}$ Å^{-2} for the three samples, respectively. Small positive values of R for all the samples show that the electron density gradient at the phase boundary is finite, suggesting that the samples belong to a non-ideal two-phase system. As proposed by Vonk,[7] for an isotropic sample the relation $R = -3(d^2C(r)/dr^2)_{r=0}$ should be valid. The values of $-3(d^2C(r)/dr^2)_{r=0}$ were computed using the five-point forward difference method and the values obtained for the three samples were $(15.5 \pm 0.01)10^{-4}$, $(12.77 \pm 0.01)10^{-4}$, and $(6.93 \pm 0.02)10^{-5}$ Å^{-2}. These values are in good agreement with R values given above indicating tht the samples are isotropic and three-dimensional correlation functions can be calculated for all of them.

Using relation (11) the three-dimensional correlation functions, $C(r)$, for all samples were computed for various values of r and are shown in Figure 3 with error bars. The slope of $C(r)$ of each sample at different points was computed by numerical differentiation applying the five-point central difference formula with a regular interval of 1 Å. The values of $-4/R(dC(r)/dr)$ *versus* r for the three samples were plotted in Figure 4, thus obtaining three curves. A straight line equidistant from both the axes was drawn for each curve and the point of intersection of this line with each curve gives the values of E referred to as E_V following the relation (12). The values of E_V obtained for three samples were 19.83 ± 0.02, 23.83 ± 0.02 and 144.0 ± 0.03 Å respectively.

Using scanning electron microscopy it was found that all the three samples have lamellar structure with limited coherence. Therefore one-dimensional correlation function, $C_1(y)$ applicable for layer structures was calculated for each sample. Using relation (14) the one-dimensional correlation functions, $C_1(y)$

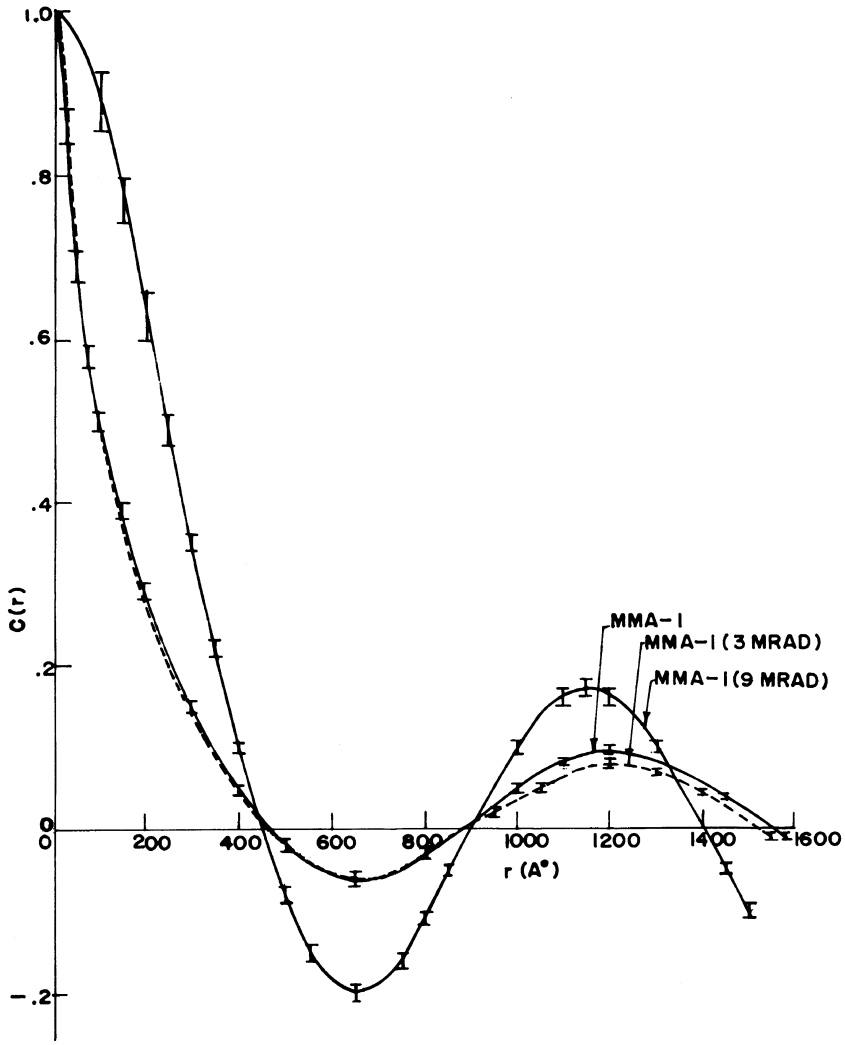

Figure 3. Curves of the three-dimensional correlation functions $C(r)$ against r-with error bars.

were computed for various values of y. The $C_1(y)$ *versus* y curves with error bars are shown in Figure 5. The values of D, periodicity transverse to the layer, were found as 945, 958, and 936 Å which were obtained by noting the position of the first subsidiary maximum in each curve in Figure 5. The 5% fluctuation in the intensity data in the case of a sample produces no change in the position of the first subsidiary maximum as verified by the computation of $C_1(y)$.

Using relation (16), the values of (S/V), area of interface per unit volume were obtained as 2.11×10^{-3}, 2.08×10^{-3}, and 2.13×10^{-3} Å^{-1}. The values of slopes $dC_1(y)/dy$ were calculated at various points greater than E_V and found to be constant ($= -0.01$, -0.01, and -0.006) for values of y from 21 Å to 30 Å, 25 Å to 34 Å, and 145 Å to 160 Å, respectively. From relation (15) the values of $\langle \Delta\eta \rangle^2/\langle \eta^2 \rangle$ were found to be 17.65 ± 3.11, 17.33 ± 3.07, and 5.91 ± 2.73, respectively. Assuming $\phi_1 + \phi_2 = 1$ and employing relation (17), the values of ϕ_1 and ϕ_2 were estimated as (0.93 ± 0.01 and 0.07 ± 0.01),

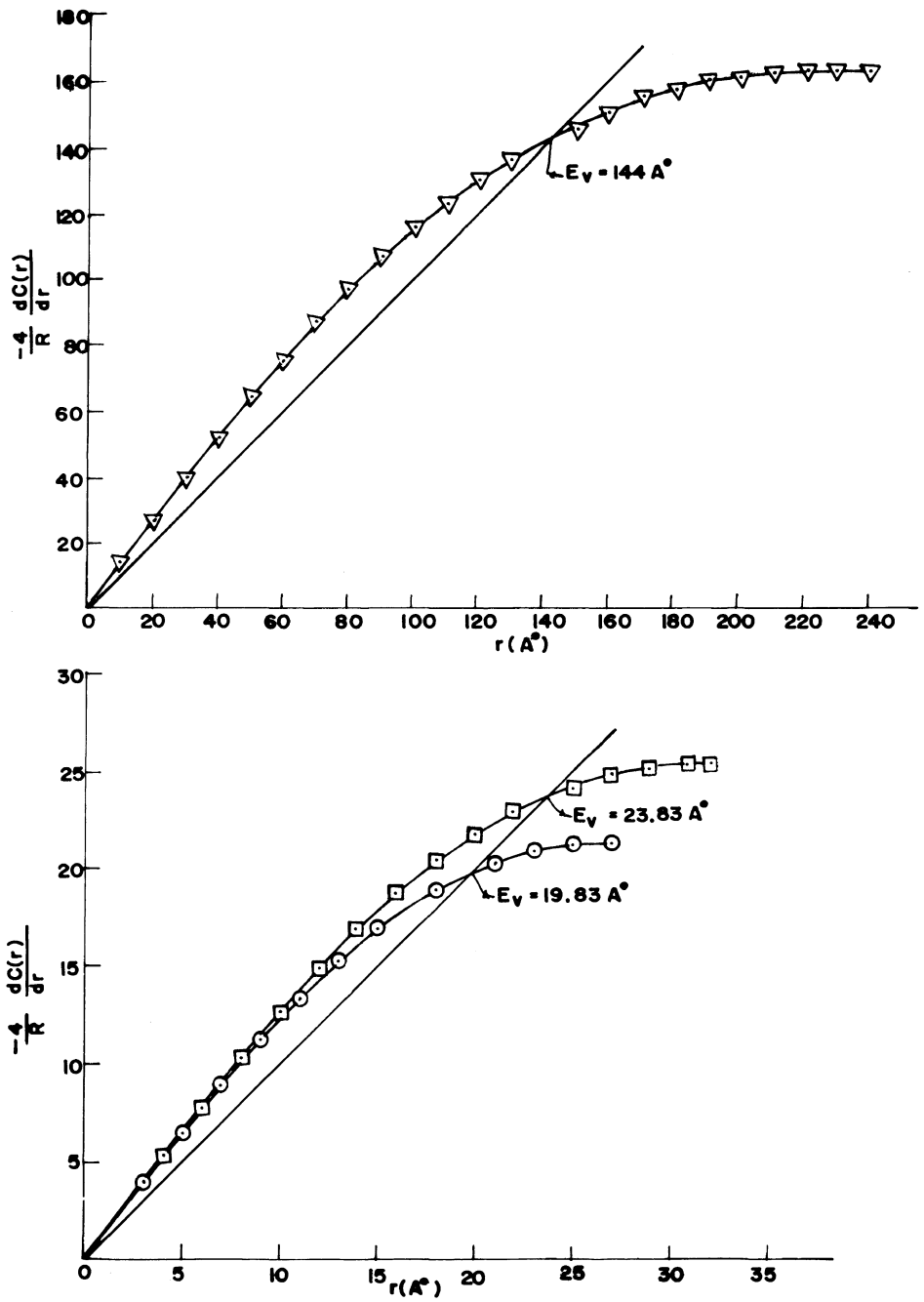

Figure 4. Curve of $-4/R$ ($dC(r)/dr$) against r. MMA-1 (open circles), MMA-1 (3 Mrad), open squares and MMA-1 (9 Mrad), reverse traingles. The straight line is equidistant from both axes.

(0.92 ± 0.01 and 0.08 ± 0.01), and (0.67 ± 0.13 and 0.33 ± 0.13), respectively. Following relation (18) the transversal lengths $\bar{l}_1$ and $\bar{l}_2$ for the three samples were found to be (1760.9 ± 19.0 and 129.0 ± 19.0 Å), (1779.9 ± 21.1 and 136.0 ± 21.1 Å), and (1258.3 ± 24.9 and $613.6 \pm$

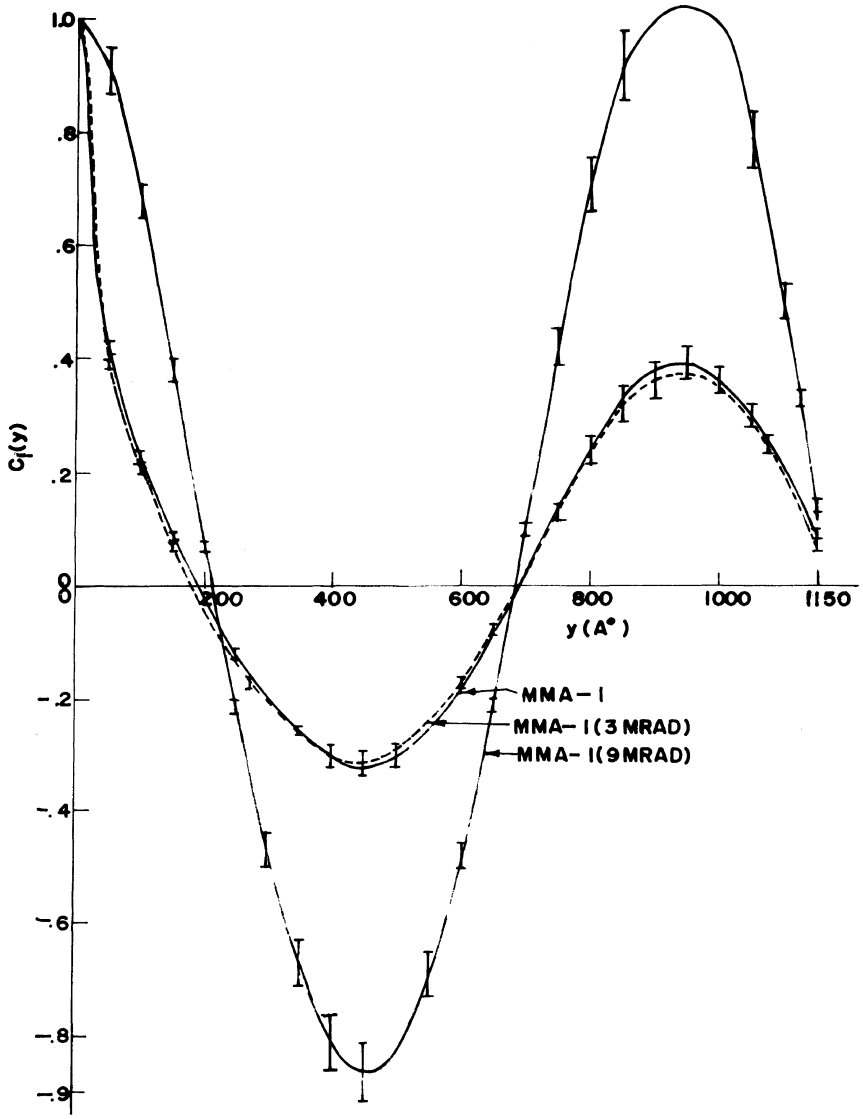

Figure 5. Curves of the one-dimensional correlation functions $C_1(y)$ against y with error bars.

24.9 Å), respectively. The range of inhomogeneity, $\bar{l}_r$ calculated from relation (19) were 120.2 ± 18.8, 126.4 ± 19.6, and 412.4 ± 21.8 Å, respectively. The lengths of coherence obtained from relation (20) were 338.0 ± 6.2, 317.9 ± 6.2, and 488.8 ± 1.5 Å. The characteristic numbers for the samples as obtained from relation (21) were 1.4 ± 0.22, 1.25 ± 0.19, and 0.59 ± 0.21, respectively. The values of $2E/D$, the volume fraction of diffuse layer were computed to be (4.19 ± 0.004), (4.97 ± 0.004), and $(30.76 \pm 0.004)\%$, respectively.

The Ruland plots, $\tilde{I}(x)x$ *versus* x^{-2} of the three samples are shown in Figure 6. The plots give straight lines at the limiting region of the scattering curves. The slopes and y intercepts were obtained from the plots as $(4.308 \pm 0.12$ and $-10.0 \pm 0.29)$, $(1.779 \pm 0.03$ and $-7.8 \pm$

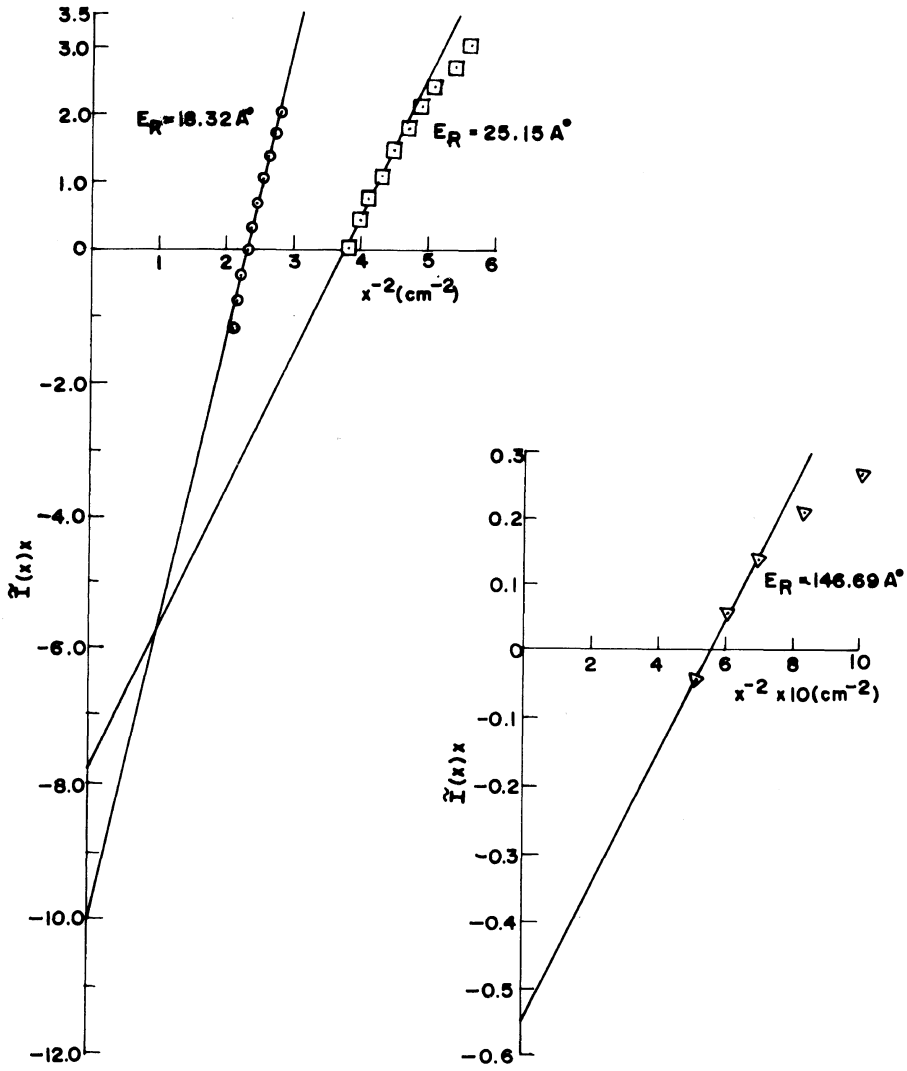

Figure 6. Ruland plot of $\tilde{I}(x)x$ *versus* x^{-2}. MMA-1 (open circles), MMA-1 (3 Mrad), open squares and MMA-1 (9 Mrad), reverse traingles.

0.01), and (0.003 ± 0.001 and -0.55 ± 0.07), respectively. Using the slope and intercept of each plot the width of the transition layer, E_R by the Ruland method were found to be 18.32 ± 1.99, 25.15 ± 0.35, and 146.69 ± 0.21 Å. Standard deviation of the intensities $\sigma(\tilde{I})^{1/2}$ was calculated at the tail region of the SAXS curve of the samples and were found to be 0.02, 0.08, and 0.03, which are well within the permissible limits. The coefficients of the line of regression were computed as 0.90, 0.94, and 0.97, respectively, indicating the correctness of the data collected.[28]

DISCUSSION

A close review of all the results shown above suggests that gamma-irradiated graft copolymers of Nylon-6 (MMA-1, MMA-1 (3 Mrad), and MMA-1 (9 Mrad)) belong to non-ideal

two-phase system. In the case of an ideal two-phase system the Ruland plot gives a straight line passing through the origin. As shown in Figure 6 the Ruland plots of the samples MMA-1, MMA-1 (3 Mrad), and MMA-1 (9 Mrad) have negative intercepts of -10.0 ± 0.29, -7.8 ± 0.01, and -0.55 ± 0.07, respectively, thereby conforming to the non-ideal two-phase nature of the samples. It may so happen that in some cases the y intercept

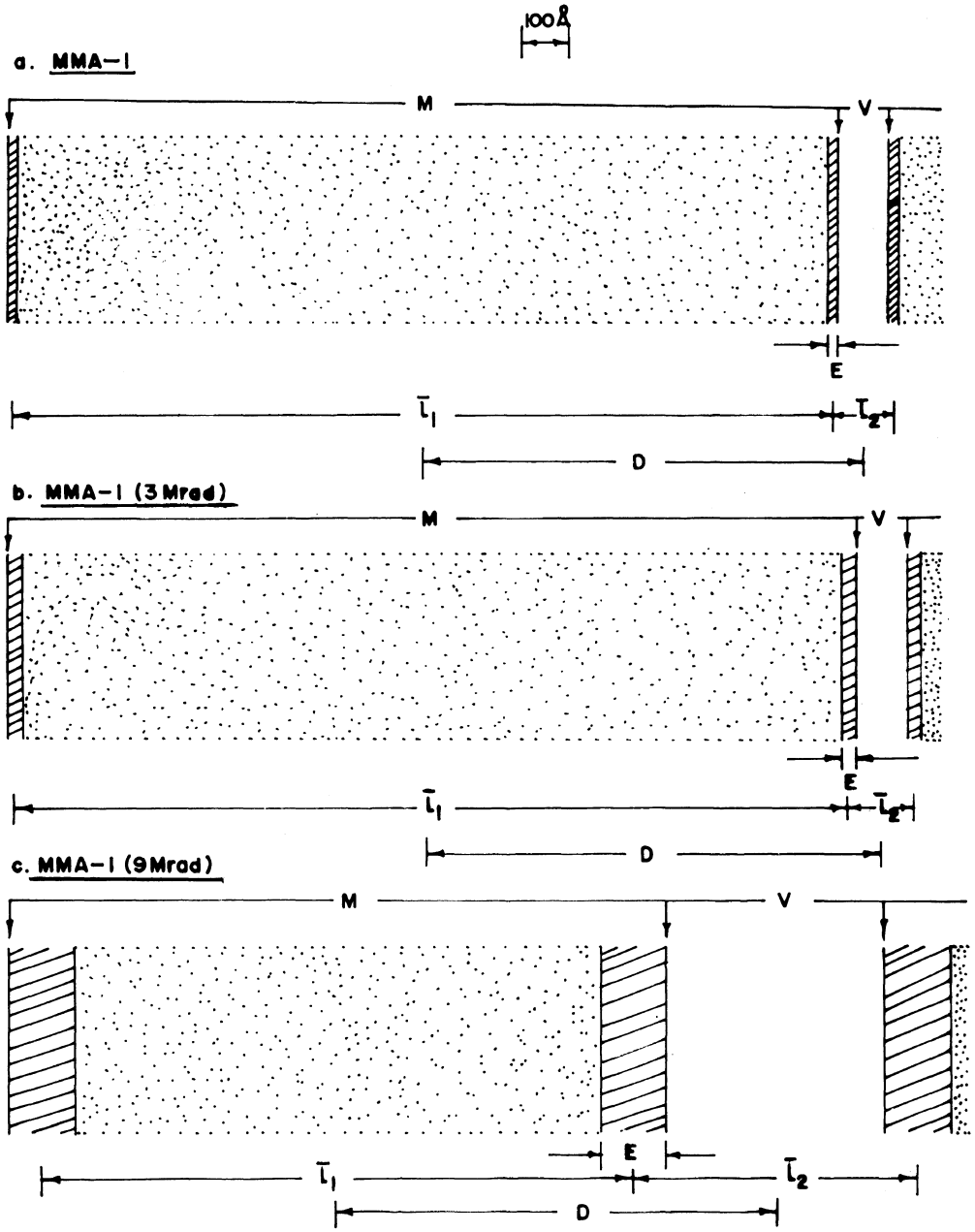

Figure 7. Lamellar model: (drawn to the scale): M, matter; V, void; D, periodicity transverse to the layer; E, width of the transition layer.

may be positive. Two possibilities may arise in such cases: the system may not be a two-phase one or the dimensions of the scattering particles may be small enough to be analyzed by SAXS.

The diffuse boundary width calculated following Vonk (E_V) and following Ruland (E_R) are found to be approximately equal for each sample. The nearly equal values obtained by two different approaches confirm the correctness of data collection and method of analysis.

The lamellar model based upon the above findings is shown in Figure 7. The $C(r)$ *versus* r plots (Figure 3) show damped oscillatory behaviour as reported by Misra *et al.*[14] for non-ideal two-phase system and the same trend is evident for all samples. Furthermore the maxima in the one-dimensional correlation functions (Figure 5) are very sharp, indicating a narrow distribution in interdomain spacing. the oscillations in the correlation functions damp out slowly, indicating a high degree of spatial coherence of the domains.

The radiation induced graft copolymerisation of methyl methacrylate (MMA) onto Nylon-6 increases steadily with increasing monomer concentration at a constant dose. This is due to complexation of the monomer (MMA) with Nylon-6 fiber.[11]

When the fibre is exposed to 3 Mrad gamma radiation the D value increases compared to MMA-1. This shows that there is cross-linking of MMA-1 with nylon substrate even in the solid state as a result of which the inter layer transverse periodicity increases and the matter phase becomes thicker (Figure 7b). However there is increase in the value of E of MMA-1 (3 Mrad) compared to MMA-1. This may be due to the fact that more MMA molecules are cross-linked to the side chain of the fibre backbone near the matter phase. When the fibre is subjected to 9 Mrad irradiation it is evident from Figure 7c that the separation between matter and matter phases increases thereby decreasing the inter layer bonding strength. The parent fibre undergoes degradation as a result of which the width of the matter phase decreases and E value increases. This leads us to assume that molecules in the transition region absorb energy from the incident gamma radiation and get separated from the parent chain of the fibre. It is further noted from Figure 2 that when MMA-1 fibres are subjected to 9 Mrad gamma-radiation, there is drastic decrease in intensity. This may be due to the break down of molecules (degradation) and is confirmed by the fact that the (S/V) value of MMA-1 (9 Mrad) increases as compared to the MMA-1 and MMA-1 (3 Mrad). Further work on this line is in progress. We will be able to predict more when the fibres are irradiated by different doses and taking different percent graft yield of the fibres.

Acknowledgments. We are thankful to Department of Science, Technology and Environment, Government of Orissa, India for providing financial assistance to one of the authors (S. S. Khuntia). We are thankful to the Principal, R. E. C., Rourkela for granting permission to use the computer and other facilities of the Physics Department. We are also thankful to Dr. K. C. Patra, Dr. D. K. Bisoyi, and Md. N. Khan for their help during the progress of the work.

REFERENCES

1. G. Porod, *Kolloid Z.*, **124**, 83 (1951); *Kolloid Z.*, **125**, 51 (1952).
2. G. Porod, *Kolloid Z.*, **125**, 108 (1952).
3. E. Helfand, *Acc. Chem. Res.*, **8**, 295 (1975).
4. E. Helfand and Y. Tagami, *Polym. Lett.*, **9**, 741 (1971).
5. S. L. Aggarwal, R. A. Livigni, L. F. Marker, and T. J. Dudek, "Block and Graft Copolymers", Syracuse University Press, New York, N.Y., 1973, p 157.
6. W. Ruland, *J. Appl. Crystallogr.*, **4**, 70 (1971).
7. C. G. Vonk, *J. Appl. Crystallogr.*, **6**, 81 (1973).
8. I. M. Trivedi and P. C. Mehta, *J. Appl. Polym. Sci.*, **19**, 14 (1975).
9. M. A. El Azmirly, A. H. Zahran, and M. F. Barakat, *Eur. Polym. J.*, **11**, 19 (1975).
10. A. A. Armstrong Jr. and H. A. Rutherford, *Text. Res. J.*, **33**, 264 (1963).

11. P. L. Nayak, S. Lenka, and A. P. Das, *Angew. Makromol. Chem.*, **131**, 187 (1985).
12. R. W. Hendricks, *J. Appl. Crystallogr.*, **3**, 348 (1970).
13. D. Caulfield and R. Ullman, *J. Appl. Phys.*, **33**, 1737 (1962).
14. T.Misra, K. C. Patra, and T. Patel, *Colloid Polym. Sci.*, **262**, 611 (1984).
15. P. Debye and A. M. Bueche, *J. Appl. Phys.*, **20**, 518 (1949).
16. J. Mering and D. Tchoubar, *J. Appl. Crystallogr.*, **1**, 153 (1968).
16a. Th. Gerber, G. Walter, and R. Kranold, *J. Appl. Cryst.*, **15**, 143 (1982).
17. G. Kortleve and C. G. Vonk, *Kolloid Z. Z. Polym.*, **225**, 124 (1968).
18. J. T. Koberstein and R. S. Stein, *J. Polym. Sci.*, **21**, 1439 (1983).
19. P. Mittelbach and G. Porod, *Kolloid Z. Z. Polym.*, **202**, 40 (1965).
20. J. Rathje and W. Ruland, *Colloid Polym. Sci.*, **254**, 358 (1976).
21. J. T. Koberstein, B. Morra and R. S. Stein, *J. Appl. Crystallogr.*, **13**, 34 (1980).
22. W. Wiegand and W. Ruland, *Prog. Colloid Polym. Sci.*, **66**, 355 (1979).
23. W. Ruland, *Colloid Polym. Sci.*, **255**, 417 (1977).
24. G. Kortleve, C. A. F. Tuynman, and C. G. Vonk, *J. Polym. Sci.*, **42**, 851 (1972).
25. G. Konrad and N. G. Zachmann, *Kolloid Z. Z. Polym.*, **247**, 851—7 (1971).
26. O. Glatter and O. Kratky, "Small Angle X-Ray Scattering, Academic, New York, N.Y., 1982, p 435.
27. C. G. Vonk, *J. Appl. Crystallogr.*, **4**, 340 (1971).
28. J. Topping, Errors of Observation and Their Treatment, 4th ed, Chapman and Hall, London, 1972.
29. C. G. Vonk, *J. Appl. Crystallogr.*, **8**, 340 (1975).